

Contents lists available at [ScienceDirect](http://ScienceDirect.com)

## Physics Letters B

[www.elsevier.com/locate/physletb](http://www.elsevier.com/locate/physletb)

# Enhanced $J/\psi$ -pair production from double-parton scatterings in nucleus–nucleus collisions at the Large Hadron Collider

David d'Enterria<sup>a,\*</sup>, Alexander M. Snigirev<sup>b</sup><sup>a</sup> CERN, PH Department, 1211 Geneva, Switzerland<sup>b</sup> Skobeltsyn Institute of Nuclear Physics, Moscow State University, 119991 Moscow, Russia

## ARTICLE INFO

## Article history:

Received 3 July 2013

Received in revised form 3 September 2013

Accepted 1 October 2013

Available online 9 October 2013

Editor: J.-P. Blaizot

## ABSTRACT

A generic expression of double-parton scattering cross sections in high-energy nucleus–nucleus (A–A) collisions is derived as a function of the corresponding single-parton hard cross sections and of the A–A event centrality. We consider the case of prompt- $J/\psi$  production in lead–lead (Pb–Pb) at the CERN Large Hadron Collider and find that about 20% (35%) of the  $J/\psi$  events in minimum-bias (most central) collisions contain a second  $J/\psi$  from double-parton interactions. In Pb–Pb at 5.5 TeV, in the absence of final-state effects, about 240 double- $J/\psi$  events are expected per unit midrapidity and per inverse-nanobarn in the dilepton decay modes. The implications of double- $J/\psi$  production on the interpretation of the observed  $J/\psi$  suppression in A–A collisions are discussed.

© 2013 Elsevier B.V. All rights reserved.

## 1. Introduction

The production of heavy-quark bound states of the charmonium ( $J/\psi$ ) and bottomonium ( $\Upsilon$ ) families in high-energy proton–proton (p–p) and nucleus–nucleus (A–A) collisions is governed by both perturbative and non-perturbative aspects of Quantum Chromodynamics (QCD) and has been extensively studied at fixed-target and collider energies [1]. For the most part, a pair of charm or bottom quarks ( $c\bar{c}$ ,  $b\bar{b}$ ) is first produced in a hard gluon–gluon collision with cross sections computable via perturbative QCD (pQCD) calculations. The subsequent evolution of the  $Q\bar{Q}$  pair towards a colour-singlet bound state is a non-perturbative process described in various theoretical approaches including colour-singlet and colour-octet mechanisms, non-relativistic QCD effective field theory, or colour evaporation models (see e.g. [2] for a review).

In the case of A–A collisions, quarkonium has been proposed as a key probe of the thermodynamical properties of the hot QCD medium produced in the course of the collision [3]. Analysis of quarkonia correlators and potentials in finite-temperature lattice QCD [4] indicate that the different  $c\bar{c}$  and  $b\bar{b}$  bound states dissociate at temperatures  $T$  for which the colour (Debye) screening radius of the medium falls below their corresponding  $Q\bar{Q}$  binding radius. Experimental confirmation of such a quarkonia dissociation pattern should provide a direct means to determine the temperature of the produced quark–gluon plasma (QGP) [5]. Surprisingly,  $J/\psi$  production in lead–lead (Pb–Pb) collisions at the

LHC [6–9] is observed to be less suppressed – compared to baseline p–p collisions at the same energy – than at the Relativistic Heavy-Ion Collider (RHIC) [10] despite the fact that the average medium temperature at LHC nucleon–nucleon centre-of-mass (c.m.) energies ( $\sqrt{s_{NN}} = 2.76$  TeV) is at least 30% higher than at RHIC ( $\sqrt{s_{NN}} = 200$  GeV) [11]. Approaches combining  $J/\psi$  dissociation in a deconfined phase plus regeneration due to charm–quark recombination [12,13] can reproduce the observed trends in the data although the model parameters ( $\sigma_{c\bar{c}}$  cross section, medium density, ...) need to be validated with other LHC observations.

In this Letter we discuss and quantify for the first time in the literature the role of double-parton scattering (DPS) processes in ultrarelativistic heavy-ion collisions, considering specifically the case of double- $J/\psi$  production in Pb–Pb at LHC energies. Due to the fast increase of the parton flux at small parton fractional momenta,  $x \equiv p_{\text{parton}}/p_{\text{hadron}}$ , the probability of having multiple hard parton interactions (MPI) occurring simultaneously at different impact parameters increases rapidly with collision energy and constitutes a significant source of particle production at semihard scales of a few GeV in p–p and, in particular, A–A collisions [14]. The evidence for DPS processes producing two independently-identified hard particles in the same collision is currently based on p–p and p– $\bar{p}$  measurements of final-states containing multi-jets, and jets plus photons [15,16] or  $W^\pm$  bosons [17] showing an excess of events in various differential distributions with respect to the expectations from contributions from single-parton scatterings (SPS) alone. LHC p–p measurements of double- $J/\psi$  production [18] as well as of single- $J/\psi$  production as a function of the event multiplicity [19] have been also interpreted in the context of DPS [20–23] and MPI models respectively.

\* Corresponding author.

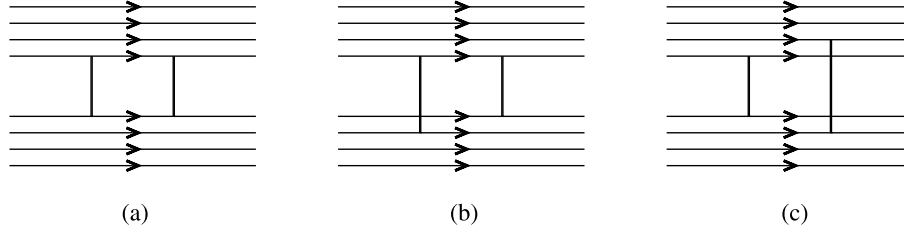


**Fig. 1.** Schematic DPS contributions in A–A collisions: (a) The two colliding partons belong to the same pair of nucleons, (b) partons from one nucleon in one nucleus collide with partons from two different nucleons in the other nucleus, and (c) the two colliding partons belong to two different nucleons from both nuclei.

We investigate DPS in A–A collisions following a similar study for p–A collisions [24], extending it to also include the centrality-dependence of the DPS cross sections. The larger transverse parton density in nuclei compared to protons results in enhanced A–A DPS contributions coming from interactions where the two partons belong or not to the same pair of nucleons of the colliding nuclei (Fig. 1). Consequently, in Pb–Pb at LHC energies we expect a non-negligible probability of two parton–parton interactions independently producing two  $J/\psi$  mesons in the same nuclear collision.

## 2. Cross sections for double-parton scattering in proton and nuclear collisions

The DPS cross section in p–p collisions can be theoretically computed from the convolution of parton distribution functions (PDF) and elementary cross sections summed over all involved partons (see e.g. [25])

$$\begin{aligned} \sigma_{(pp \rightarrow ab)}^{\text{DPS}} &= \left(\frac{m}{2}\right) \sum_{i,j,k,l} \int \Gamma_p^{ij}(x_1, x_2; \mathbf{b}_1, \mathbf{b}_2; Q_1^2, Q_2^2) \\ &\times \hat{\sigma}_a^{ik}(x_1, x'_1; Q_1^2) \hat{\sigma}_b^{jl}(x_2, x'_2; Q_2^2) \\ &\times \Gamma_p^{kl}(x'_1, x'_2; \mathbf{b}_1 - \mathbf{b}, \mathbf{b}_2 - \mathbf{b}; Q_1^2, Q_2^2) dx_1 dx_2 dx'_1 dx'_2 d^2 b_1 d^2 b_2 d^2 b, \end{aligned} \quad (1)$$

where  $\Gamma_p^{ij}(x_1, x_2; \mathbf{b}_1, \mathbf{b}_2; Q_1^2, Q_2^2)$  are double-PDF which depend on the longitudinal momentum fractions  $x_1$  and  $x_2$  and transverse positions  $\mathbf{b}_1$  and  $\mathbf{b}_2$  of the two partons undergoing the hard processes at scales  $Q_1$  and  $Q_2$ ,  $\hat{\sigma}_a^{ik}$  and  $\hat{\sigma}_b^{jl}$  are the parton-level subprocess cross sections, and  $\mathbf{b}$  is the impact parameter vector connecting the centres of the colliding protons in the transverse plane. The combinatorial factor  $m/2$  accounts for indistinguishable ( $m=1$ ) and distinguishable ( $m=2$ ) final-states. In a model-independent way, the cross section of double-parton scattering can be expressed in the simple generic form

$$\sigma_{(pp \rightarrow ab)}^{\text{DPS}} = \left(\frac{m}{2}\right) \frac{\sigma_{(pp \rightarrow a)}^{\text{SPS}} \cdot \sigma_{(pp \rightarrow b)}^{\text{SPS}}}{\sigma_{\text{eff,pp}}}, \quad (2)$$

where  $\sigma^{\text{SPS}}$  is the inclusive single-hard scattering cross section, computable perturbatively to a given order in  $\alpha_s$ ,

$$\begin{aligned} \sigma_{(pp \rightarrow a)}^{\text{SPS}} &= \sum_{i,k} \int D_p^i(x_1; Q_1^2) f(\mathbf{b}_1) \hat{\sigma}_a^{ik}(x_1, x'_1) \\ &\times D_p^k(x'_1; Q_1^2) f(\mathbf{b}_1 - \mathbf{b}) dx_1 dx'_1 d^2 b_1 d^2 b \\ &= \sum_{i,k} \int D_p^i(x_1; Q_1^2) \hat{\sigma}_a^{ik}(x_1, x'_1) D_p^k(x'_1; Q_1^2) dx_1 dx'_1, \end{aligned} \quad (3)$$

and  $\sigma_{\text{eff,pp}}$  is a normalisation cross section that encodes all “DPS unknowns” into a single parameter which can be experimentally measured. A numerical value,  $\sigma_{\text{eff,pp}} \approx 14$  mb, has been obtained

empirically from fits to p–p and p– $\bar{p}$  data [15–17]. One can identify  $\sigma_{\text{eff,pp}}$  with the inverse of the proton overlap function squared:  $\sigma_{\text{eff,pp}} = [\int d^2 b t^2(\mathbf{b})]^{-1}$  under the two following simplifying approximations: (i) the double-PDF can be decomposed into longitudinal and transverse components, with the latter expressed in terms of the overlap function  $t(\mathbf{b}) = \int f(\mathbf{b}_1) f(\mathbf{b}_1 - \mathbf{b}) d^2 b_1$  for a given parton transverse thickness function  $f(\mathbf{b})$  representing the effective transverse overlap area of partonic interactions that produce the DPS process, and (ii) the longitudinal component reduces to the “diagonal” product of two independent single-PDF,  $D_p^i(x_1; Q_1^2)$ .

To compute the DPS cross section in nucleus–nucleus collisions we proceed as done for p–A in [24]. The parton flux is enhanced by the number  $A$  of nucleons in each nucleus and the single-parton cross section is simply expected to be that of p–p – or, more exactly, nucleon–nucleon (N–N) collisions taking into account shadowing effects in the nuclear PDF (see below) – scaled by the factor  $A^2$ , i.e.

$$\begin{aligned} \sigma_{(AA \rightarrow a)}^{\text{SPS}} &= \sigma_{(NN \rightarrow a)}^{\text{SPS}} \int T_A(\mathbf{b}_1) T_A(\mathbf{b}_1 - \mathbf{b}) d^2 b_1 d^2 b \\ &= \sigma_{(NN \rightarrow a)}^{\text{SPS}} \int T_{AA}(\mathbf{b}) d^2 b = A^2 \cdot \sigma_{(NN \rightarrow a)}^{\text{SPS}}. \end{aligned} \quad (4)$$

Here  $T_A(\mathbf{b})$  is the nuclear thickness function at impact parameter vector  $\mathbf{b}$  connecting the centres of the colliding nucleus in the transverse plane, and  $T_{AA}(\mathbf{b})$  the standard nuclear overlap function normalised to  $A^2$  [26]. The DPS A–A cross section is thus the sum of three terms, corresponding to the diagrams of Fig. 1:

1. The first term corresponding to Fig. 1(a) is just, similarly to the SPS cross sections Eq. (4), the DPS cross section in N–N collisions scaled by  $A^2$

$$\sigma_{(AA \rightarrow ab)}^{\text{DPS,1}} = A^2 \cdot \sigma_{(NN \rightarrow ab)}^{\text{DPS}}. \quad (5)$$

2. The second term, Fig. 1(b), accounts for interactions with partons from one nucleon in one nucleus with partons from two different nucleons in the other nucleus. This term was originally derived in [27] in the context of p–A collisions,

$$\sigma_{(AA \rightarrow ab)}^{\text{DPS,2}} = 2 \sigma_{(NN \rightarrow ab)}^{\text{DPS}} \cdot \sigma_{\text{eff,pp}} \cdot T_{2,AA}, \quad (6)$$

with

$$\begin{aligned} T_{2,AA} &= \frac{A-1}{A} \int T_A(\mathbf{b}_1) T_A(\mathbf{b}_1 - \mathbf{b}) T_A(\mathbf{b}_1 - \mathbf{b}) d^2 b_1 d^2 b \\ &= (A-1) \int d^2 r T_A^2(\mathbf{r}) = (A-1) \cdot T_{AA}(0). \end{aligned} \quad (7)$$

3. The third contribution from interactions of partons from two different nucleon in one nucleus with partons from two different nucleons in the other nucleus, Fig. 1(c), reads

$$\sigma_{(AA \rightarrow ab)}^{\text{DPS,3}} = \sigma_{(NN \rightarrow ab)}^{\text{DPS}} \cdot \sigma_{\text{eff,pp}} \cdot T_{3,AA}, \quad (8)$$

with

$$\begin{aligned} T_{3,AA} &= \left(\frac{A-1}{A}\right)^2 \int T_A(\mathbf{b}_1)T_A(\mathbf{b}_2)T_A(\mathbf{b}_1-\mathbf{b}) \\ &\quad \times T_A(\mathbf{b}_2-\mathbf{b}) d^2b_1 d^2b_2 d^2b \\ &= \left(\frac{A-1}{A}\right)^2 \int d^2r T_{AA}^2(\mathbf{r}), \end{aligned} \quad (9)$$

where the integral of the nuclear overlap function squared does not depend much on the precise shape of the transverse parton density in the nucleus, amounting to  $A^2/1.94 \cdot T_{AA}(0)$  for a hard-sphere and  $A^2/2 \cdot T_{AA}(0)$  for a Gaussian profile.

The factors  $(A-1)/A$  and  $[(A-1)/A]^2$  in the two last terms take into account the difference between the number of nucleon pairs and the number of *different* nucleon pairs. Adding (5), (6) and (8), the inclusive cross section of a DPS process with two hard parton subprocesses  $a$  and  $b$  in A–A collisions (with  $A$  large, so that  $A-1 \approx A$ ) can be written as

$$\begin{aligned} \sigma_{(AA \rightarrow ab)}^{\text{DPS}} &= A^2 \sigma_{(NN \rightarrow ab)}^{\text{DPS}} \cdot \left[ 1 + \frac{2(A-1)}{A^2} \sigma_{\text{eff,pp}} \int d^2r T_A^2(\mathbf{r}) \right. \\ &\quad \left. + \left(\frac{A-1}{A^2}\right)^2 \sigma_{\text{eff,pp}} \int d^2r T_{AA}^2(\mathbf{r}) \right] \quad (10) \\ &\approx A^2 \sigma_{(NN \rightarrow ab)}^{\text{DPS}} \cdot \left[ 1 + \frac{2}{A} \sigma_{\text{eff,pp}} T_{AA}(0) \right. \\ &\quad \left. + \frac{1}{2} \sigma_{\text{eff,pp}} T_{AA}(0) \right], \quad (11) \end{aligned}$$

where the term in parentheses follows a dependence of the type  $A^{4/3}/6$  and thus  $\sigma^{\text{DPS}}$  in A–A increases roughly as  $A^{3.3}/5$  compared to its value in p–p collisions. The DPS cross sections in A–A are practically unaffected by the value of  $\sigma_{\text{eff,pp}}$  but dominated instead by double-parton interactions from different nucleons in both nuclei, and thus less sensitive to possible extra “non-diagonal” parton interference terms [27], computed for light nuclei in [28].

For  $^{208}\text{Pb}$ – $^{208}\text{Pb}$  collisions, in the simplest hard-sphere approximation for a uniform density of radius  $R_A = r_0 A^{1/3}$  and  $r_0 = 1.25$  fm, the nuclear overlap function at  $b=0$  is  $T_{AA}(0) = 9A^2/(8\pi R_A^2) = 31.5 \text{ mb}^{-1}$ . A direct evaluation of the integral using the measured Fermi–Dirac spatial density for the Pb nucleus ( $R_A = 6.624$  fm and surface thickness  $a = 0.546$  fm) [29] yields  $T_{AA}(0) = 30.4 \text{ mb}^{-1}$ . Using the latter  $T_{AA}(0)$  value and  $\sigma_{\text{eff,pp}} = 14$  mb, the expression in parentheses in Eq. (11) – which quantifies the total DPS enhancement factor in A–A compared to N–N collisions, Eq. (5) – is found to be of the order of 200, dominated by the hard double-nucleon scattering contributions, Fig. 1(c). The final DPS cross section “pocket formula” in nucleus–nucleus collisions can be obtained combining Eqs. (2) and (11):

$$\sigma_{(AA \rightarrow ab)}^{\text{DPS}} = \left(\frac{m}{2}\right) \frac{\sigma_{(NN \rightarrow a)}^{\text{SPS}} \cdot \sigma_{(NN \rightarrow b)}^{\text{SPS}}}{\sigma_{\text{eff,AA}}}, \quad (12)$$

with the effective A–A normalisation cross section for Pb–Pb amounting to

$$\sigma_{\text{eff,AA}} = \frac{1}{A^2[\sigma_{\text{eff,pp}}^{-1} + \frac{2}{A}T_{AA}(0) + \frac{1}{2}T_{AA}(0)]} = 1.5 \text{ nb}. \quad (13)$$

The relative contributions of the three terms in the denominator, corresponding to the diagrams of Fig. 1, are approximately 1:4:200. We note that Eq. (13) is valid only for pQCD processes with cross sections  $\sigma_{(NN \rightarrow a)}^{\text{SPS}}$  smaller than about  $A^2 \sigma_{\text{eff,AA}}$  (which holds for the

$J/\psi$  case of interest here), otherwise one would need to reinterpret it to account for triple (and higher-multiplicity) parton scatterings. Numerically we see that whereas the single-parton cross sections in Pb–Pb collisions, Eq. (4), are enhanced by a factor of  $A^2 \simeq 4 \cdot 10^4$  compared to that in p–p collisions, the corresponding double-parton cross sections are enhanced by a much higher factor of  $\sigma_{\text{eff,pp}}/\sigma_{\text{eff,AA}} \propto A^{3.3}/5 \simeq 9 \cdot 10^6$ .

### 3. Centrality-dependence of the DPS cross sections

The cross sections discussed so far are for “minimum-bias” (MB) A–A collisions without any selection in the reaction centrality. The cross sections for single- and double-parton scattering within an interval of impact parameters  $[b_1, b_2]$ , corresponding to a given centrality percentile,  $f\%$  = 0–100%, of the total A–A cross section  $\sigma_{AA}$ , with average nuclear overlap function  $\langle T_{AA}[b_1, b_2] \rangle$  are

$$\begin{aligned} \sigma_{(AA \rightarrow a)}^{\text{SPS}}[b_1, b_2] &= A^2 \cdot \sigma_{(NN \rightarrow a)}^{\text{SPS}} \cdot f_1[b_1, b_2] \\ &= \sigma_{(NN \rightarrow a)}^{\text{SPS}} \cdot f\% \sigma_{AA} \cdot \langle T_{AA}[b_1, b_2] \rangle, \end{aligned} \quad (14)$$

$$\begin{aligned} \sigma_{(AA \rightarrow ab)}^{\text{DPS}}[b_1, b_2] &= A^2 \cdot \sigma_{(NN \rightarrow ab)}^{\text{DPS}} \cdot f_1[b_1, b_2] \\ &\quad \times \left[ 1 + \frac{2}{A} \sigma_{\text{eff,pp}} T_{AA}(0) \frac{f_2[b_1, b_2]}{f_1[b_1, b_2]} \right. \\ &\quad \left. + \sigma_{\text{eff,pp}} T_{AA}(0) \frac{f_3[b_1, b_2]}{f_1[b_1, b_2]} \right], \end{aligned} \quad (15)$$

where the latter has been obtained integrating Eq. (10) over  $b_1 < b < b_2$  and where the three dimensionless and appropriately-normalised fractions  $f_1$ ,  $f_2$ , and  $f_3$  read

$$f_1[b_1, b_2] = \frac{2\pi}{A^2} \int_{b_1}^{b_2} b db T_{AA}(b) = \frac{f\% \sigma_{AA}}{A^2} \langle T_{AA}[b_1, b_2] \rangle,$$

$$\begin{aligned} f_2[b_1, b_2] &= \frac{2\pi}{AT_{AA}(0)} \int_{b_1}^{b_2} b db \\ &\quad \times \int d^2b_1 T_A(\mathbf{b}_1)T_A(\mathbf{b}_1-\mathbf{b})T_A(\mathbf{b}_1-\mathbf{b}), \end{aligned}$$

$$f_3[b_1, b_2] = \frac{2\pi}{A^2 T_{AA}(0)} \int_{b_1}^{b_2} b db T_{AA}^2(b).$$

We can evaluate the integrals  $f_2$ , and  $f_3$  for small enough centrality bins around a given impact parameter  $b$ . The dominant  $f_3/f_1$  contribution in Eq. (15) is simply given by the ratio  $\langle T_{AA}[b_1, b_2] \rangle / T_{AA}(0)$  which is practically insensitive (except for very peripheral collisions) to the precise shape of the nucleon density in the nucleus [30]. The second centrality-dependent DPS term,  $f_2/f_1$ , cannot be expressed in a simple form in terms of  $T_{AA}(b)$ . It is of order unity for the most central collisions ( $b=0$ ),  $f_2/f_1 = 4/3-16/15$  for Gaussian and hard-sphere profiles respectively, but it is suppressed in comparison with the third leading term by an extra factor  $\sim 2/A$ . For not very peripheral collisions ( $f\% \lesssim 0-65\%$ ), the DPS cross section in a (thin) impact-parameter range can be approximated by

$$\begin{aligned} \sigma_{(AA \rightarrow ab)}^{\text{DPS}}[b_1, b_2] &\approx \sigma_{(NN \rightarrow ab)}^{\text{DPS}} \cdot \sigma_{\text{eff,pp}} \cdot f\% \sigma_{AA} \cdot \langle T_{AA}[b_1, b_2] \rangle^2 \\ &= \left(\frac{m}{2}\right) \sigma_{(NN \rightarrow a)}^{\text{SPS}} \cdot \sigma_{(NN \rightarrow b)}^{\text{SPS}} \cdot f\% \sigma_{AA} \\ &\quad \cdot \langle T_{AA}[b_1, b_2] \rangle^2. \end{aligned} \quad (16)$$

**Table 1**  
Total cross sections at LHC energies for the production of prompt- $J/\psi$  in single-parton scatterings (SPS) in p-p, N-N, Pb-Pb collisions, and of prompt- $J/\psi$ -pairs in double-parton scatterings (DPS) in Pb-Pb. The p-p values are extrapolated from experimental data, the N-N values are an NLO CEM prediction including EPS09 nuclear PDFs, and the Pb-Pb results are derived from the N-N cross sections via the quoted equations.

Process	Cross section	$\sqrt{s_{NN}}$ (TeV)			
		1.96	2.76	5.5	7.0
$\sigma^{\text{SPS}}(\text{p-p, p-}\bar{\text{p}} \rightarrow J/\psi X)$ [ $\mu\text{b}$ ]	measured (extrapolated)	$25. \pm 9.$	$28. \pm 8.$	–	$49. \pm 9.$
$\sigma^{\text{SPS}}(\text{N-N} \rightarrow J/\psi X)$ [ $\mu\text{b}$ ]	CEM(NLO) + EPS09 PDF, Eq. (3)	$14. \pm 4.$	$16. \pm 3.$	$25. \pm 5.$	$29. \pm 6.$
$\sigma^{\text{SPS}}(\text{Pb-Pb} \rightarrow J/\psi X)$ [mb]	Eq. (4)	$600 \pm 140$	$700 \pm 150$	$1100 \pm 250$	$1250 \pm 280$
$\sigma^{\text{DPS}}(\text{Pb-Pb} \rightarrow J/\psi J/\psi X)$ [mb]	Eqs. (12)–(13)	$65 \pm 15$	$90 \pm 20$	$200 \pm 50$	$270 \pm 60$

Taking the ratio of this expression over Eq. (14), one obtains the corresponding ratio of double to single-parton scattering cross sections as a function of impact parameter:

$$\left(\frac{\sigma_{(AA \rightarrow ab)}^{\text{DPS}}}{\sigma_{(AA \rightarrow a)}^{\text{SPS}}}\right)[b_1, b_2] \approx \left(\frac{m}{2}\right) \sigma_{(\text{NN} \rightarrow b)}^{\text{SPS}} \cdot \langle T_{AA}[b_1, b_2] \rangle. \quad (17)$$

This analytical expression neglects the first and second terms of Eq. (15). In the centrality percentile  $f_{\%} \approx 65$ –100% the second term would add about 20% more DPS cross sections, and for very peripheral collisions ( $f_{\%} \approx 85$ –100%, where  $\langle T_{AA}[b_1, b_2] \rangle$  is of order or less than  $1/\sigma_{\text{eff,pp}}$ ) the contributions from the first term are also non-negligible.

#### 4. Results

From Eqs. (12), with  $m = 1$ , and (13) we can compute the expected double-parton cross sections for  $J/\psi$ -pair production in Pb-Pb from the single-parton  $J/\psi$  cross sections in nucleon-nucleon collisions,  $\sigma_{(\text{NN} \rightarrow J/\psi X)}^{\text{SPS}}$ , obtained with the colour evaporation model (CEM) [31] cross-checked with the existing p-p and p- $\bar{p}$  Tevatron and LHC data, and taking into account nuclear PDF modifications [32]. The SPS cross sections for prompt- $J/\psi$ , after subtraction of the decay contributions from bottom mesons, have been measured down to zero  $p_T$  in p- $\bar{p}$  at  $\sqrt{s} = 1.96$  TeV at rapidities  $|y| < 0.6$  [33] and in p-p at  $\sqrt{s} = 2.76$  TeV ( $|y| < 0.9$  [34],  $2 < |y| < 4.5$  [35]) and 7 TeV ( $|y| < 0.9$  [36],  $1.6 < |y| < 2.4$  [37],  $2 < |y| < 4.5$  [38]). Empirical extrapolations to total  $J/\psi$  cross sections at the LHC can be obtained by integrating a Gaussian distribution fitted to the data points measured at different  $y$ . The Tevatron midrapidity cross section can be extrapolated to full-rapidity with the prescription of [39]. The values obtained, with their propagated uncertainties, are listed in Table 1 and shown as data points in Fig. 2 (top) as a function of the c.m. energy. Recent next-to-leading-order (NLO) CEM predictions for  $\sigma_{(\text{pp} \rightarrow J/\psi X)}^{\text{SPS}}$  with theoretical scales  $\mu_F = 1.5m_c$  and  $\mu_R = 1.5m_c$  for a  $c$ -quark mass  $m_c = 1.27$  GeV (solid curve) [40], agree well with the experimental data including a  $\pm 20\%$  uncertainty from the scales. The corresponding values for  $\sigma_{(\text{NN} \rightarrow J/\psi X)}^{\text{SPS}}$  are obtained from the CEM p-p cross sections scaled by the NLO EPS09 nuclear PDF shadowing. In the relevant  $(x, Q^2) \approx (10^{-3}, m_{J/\psi}^2)$  region, the Pb gluon PDF is moderately depleted, by a factor of  $(1 - S_{g,\text{Pb}}) \approx 10\%$ –20% with respect to the free nucleon density, resulting in a reduction of the  $gg \rightarrow J/\psi + X$  yields by a factor of  $(1 - S_{g,\text{Pb}}^2) \approx 20\%$ –35% (dashed-dotted line in Fig. 2, top). The EPS09 uncertainties, of the order of  $\pm 10$ –15%, have been propagated in quadrature with those associated with the theoretical scales, into the N-N cross sections. We note that the EPS09 parametrisation is clearly favoured by the  $J/\psi$  photoproduction data measured by ALICE in ultraperipheral Pb-Pb collisions at 2.76 TeV [41].

The two uppermost curves in the top panel of Fig. 2 show the resulting Pb-Pb cross sections for single- and double- $J/\psi$  production, whereas their ratio is shown in the bottom panel. At the nominal Pb-Pb energy of 5.5 TeV, single prompt- $J/\psi$  cross sec-

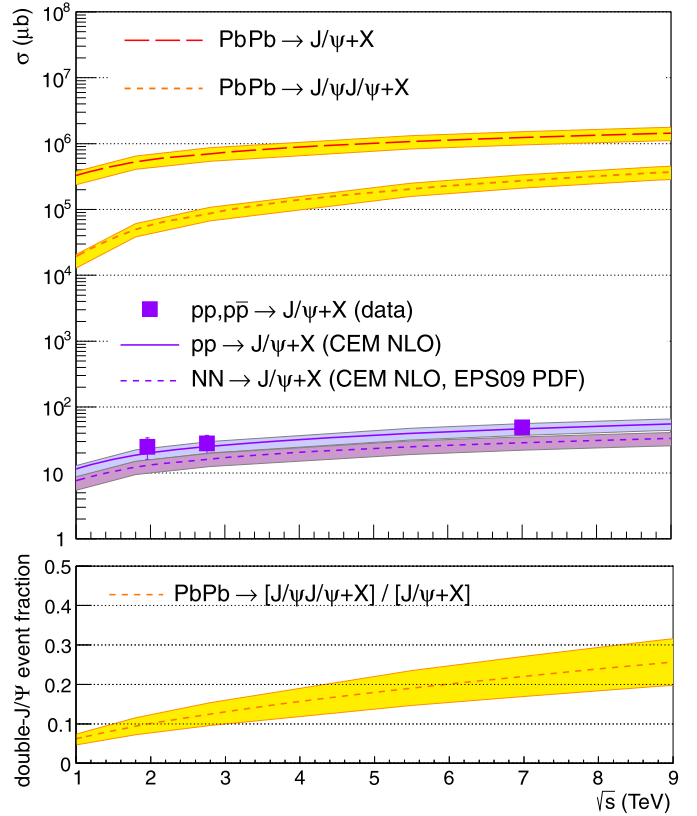


**Fig. 2.** Top: Cross sections for prompt- $J/\psi$  production in p-p, N-N, and Pb-Pb collisions and for double-parton  $J/\psi J/\psi$  in Pb-Pb, as a function of c.m. energy. Bottom: Fraction of prompt- $J/\psi$  events where a pair of  $J/\psi$  is produced in Pb-Pb collisions, as a function of c.m. energy. The bands show the nuclear PDF and scales uncertainties in quadrature. (For interpretation of the references to colour, the reader is referred to the web version of this Letter.)

tions (dashed curve) amount to about 1 b, and  $\sim 20\%$  of such collisions are actually accompanied by the production of a second  $J/\psi$  from a double-parton interaction (dotted curve), whereas such processes are negligible at RHIC energies. The rise of the DPS/SPS ratio tends to slow down at higher  $\sqrt{s_{NN}}$  as the nuclear PDF shadowing (which enters squared in the numerator but only linearly in the denominator) increases, thereby reducing the total double- $J/\psi$  yields. The yellow bands in Fig. 2, amounting to about  $\pm 25\%$ , include in quadrature the EPS09 PDF and theoretical scales uncertainties.

The ratio of single- to double- $J/\psi$  production, Eq. (17), as a function of the reaction centrality quantified by the number of participant nucleons ( $0 < N_{\text{part}} < 2A$ ) in Pb-Pb at 5.5 TeV is shown in Fig. 3. The probability of  $J/\psi$ -pair production increases rapidly and at the highest centralities (lowest impact parameters), about 35% of the Pb-Pb  $\rightarrow J/\psi + X$  collisions have a second  $J/\psi$  in the final-state. We note that the DPS cross sections have to be understood



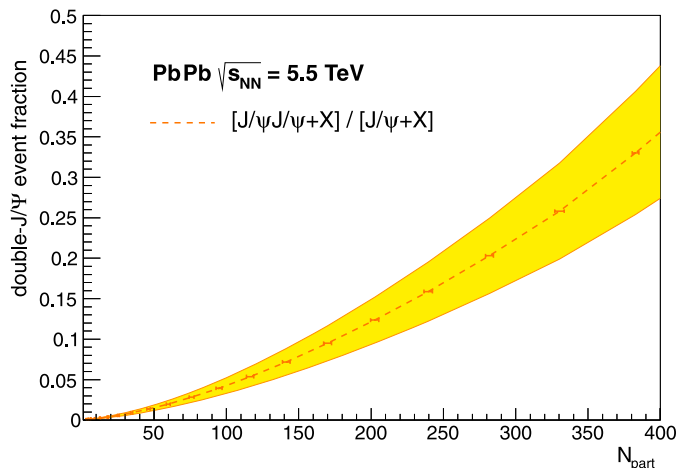


**Fig. 3.** Fraction of prompt- $J/\psi$  events in Pb–Pb collisions at 5.5 TeV where a  $J/\psi$ -pair is produced from double-parton scatterings as a function of the reaction centrality (given by  $N_{\text{part}}$ ), according to Eq. (17). The band shows the EPS09 PDF plus scale uncertainties.

as inclusive values, but they do not represent an extra contribution to the total prompt- $J/\psi$  rates since they are already part of the Pb–Pb  $\rightarrow J/\psi + X$  cross section.

Our predictions can be experimentally confirmed by measuring the cross sections for the simultaneous production of two  $J/\psi$  mesons in the same Pb–Pb event via their visible dilepton decay channels. The two  $J/\psi$  mesons issuing from double-parton scatterings have on average identical  $p_T$  and  $y$  distributions. At LHC energies, the cross section per unit-rapidity for single- $J/\psi$  amounts to  $d\sigma_{J/\psi}/dy \approx \sigma_{J/\psi}/8$  at the (low- $p_T$ ) rapidities covered by ALICE (at  $y = 0$ ) and CMS (at  $y = 2$ ), the detector acceptance and reconstruction efficiencies reduce the measured yield by factors of  $\sim 12$ – $14$  [9,37], and the dilepton branching ratio amounts to about 6%. Squaring all these quantities for the case of  $J/\psi$ -pair production results in a final reduction factor of order  $3 \cdot 10^{-7}$  for both rapidity ranges. Thus, at 5.5 TeV one would expect a visible DPS cross section of about  $d\sigma_{J/\psi J/\psi}^{\text{DPS}}/dy|_{y=0.2} \approx 60$  nb per dilepton decay mode, i.e. about 240 double- $J/\psi$  events per unit-rapidity in the four combinations of dielectron and dimuon channels in  $1 \text{ nb}^{-1}$  of integrated luminosity, assuming no in-medium suppression (accounting for it would reduce the yields by a two-fold factor, see below). The same estimates for the 15 (150)  $\mu\text{b}^{-1}$  of Pb–Pb data already collected at 2.76 TeV result in about 3.5 (35) double- $J/\psi$  events in ALICE (CMS) per unit- $y$  at mid (forward) rapidity. The combinatorial background of dilepton pairs with invariant masses around  $m_{J/\psi}$  needs to be taken into account in order to carry out such a measurement on an event-by-event basis.

## 5. Discussion and conclusions

The Pb–Pb cross sections discussed so far include initial-state nuclear PDF modifications but no final-state effects which can modify the final measured yields. Experimentally, Pb–Pb collisions at 2.76 TeV show a two-fold reduction of the MB  $J/\psi$  yields with respect to p–p, i.e.  $R_{\text{AA}}^{\text{MB}} = \sigma_{\text{AA}}/(A^2 \cdot \sigma_{\text{pp}}) \approx 0.5$ , whereas the corresponding value amounts to  $R_{\text{AA}}^{\text{MB}} \approx 0.4$  at RHIC. In central Pb–Pb collisions, the  $J/\psi$  yields at the LHC are even less depleted ( $R_{\text{AA}}^{\text{cent}} \approx 0.5$ ) than at RHIC ( $R_{\text{AA}}^{\text{cent}} \approx 0.2$ – $0.3$ ). Assuming that the dominant suppression at both energies is due to the “melting” of the  $J/\psi$  state in the QGP, the smaller LHC suppression has been interpreted as indicative of a new component of regenerated  $J/\psi$  from  $c\bar{c}$  recombination [12,13], accounting for up

to 30% of the final production. Such an additional contribution has nothing to do with the primordial DPS processes discussed here which, as aforementioned, are already accounted for in the total A–A prompt- $J/\psi + X$  yields. In particular, suppression due to colour deconfinement in the plasma should, on average, affect equally the doubly-produced  $J/\psi$ 's and, thus, the overall  $R_{\text{AA}}$  suppression factor should remain the same independently if the  $J/\psi$ 's are produced in the same or in two different Pb–Pb collisions. Reciprocally, our results demonstrate that the observation of double (or higher-multiplicity)  $J/\psi$  production in a given Pb–Pb event should not be wrongly interpreted as indicative of extra contributions from regenerated  $J/\psi$ 's, as DPS processes are an intrinsic component of the total  $J/\psi$  production with or without final-state QGP effects. Such a standard assumption is quantitatively substantiated in this work for the first time. Differentiating  $J/\psi$  from double-parton scatterings and from plasma regeneration is possible making use of their different kinematical distributions. Whereas,  $J/\psi$  from DPS have on average identical  $p_T$  and  $y$  distributions as those SPS-produced, the  $J/\psi$  coming from coalescence of thermal  $c\bar{c}$  pairs have softer  $p_T$  and are relatively more produced at central than forward rapidities as the  $c\bar{c}$  density is larger at  $y = 0$  and the regenerated yields scale with the density squared.

In summary, we have derived a simple generic expression for double-parton scattering (DPS) cross sections in heavy-ion collisions as a function of the elementary single-parton cross sections in nucleon–nucleon collisions, and an effective  $\sigma_{\text{eff,AA}}$  parameter dependent on the transverse profile of the system. The DPS cross sections in A–A are found to be enhanced by a factor of  $A^{3.3}/5$ , to be compared with the  $A^2$ -scaling of single-parton scatterings. We have studied the case of  $J/\psi$ -pair production at LHC energies and found that DPS constitute an important fraction of the total prompt- $J/\psi$  cross sections, amounting to 20% (35%) of the primordial production in minimum-bias (most central) Pb–Pb collisions. At 5.5 TeV, about 240 double- $J/\psi$  events are expected per unit-rapidity in the dilepton decay channels (in the absence of final-state suppression) for an integrated luminosity of  $1 \text{ nb}^{-1}$ , providing a quantitative test of the predictions presented here. Pair-production of pQCD probes issuing from double-parton scatterings represents an important feature of heavy-ion collisions at the LHC and needs to be taken into account in any attempt to fully understand the event-by-event characteristics of any yield suppression and/or enhancement observed in Pb–Pb compared to p–p data.

## Acknowledgements

We are grateful to T. Dahms, J.Ph. Lansberg, I. Lokhtin, G. Martinez, C. Suiere and H. Woehri for useful discussions, to R. Vogt for providing the latest CEM predictions, and in particular to A. Morsch for corrections to a previous version of this Letter as well as for valuable quantitative cross checks of the results presented here. This work is partly supported by the CERN-RFBR Joint Research Grant No. 12-02-91505.

## References

- [1] N. Brambilla, et al., Eur. Phys. J. C 71 (2011) 1534.
- [2] J.P. Lansberg, Int. J. Mod. Phys. A 21 (2006) 3857.
- [3] T. Matsui, H. Satz, Phys. Lett. B 178 (1986) 416.
- [4] S. Datta, F. Karsch, P. Petreczky, I. Wetzorke, Phys. Rev. D 69 (2004) 094507.
- [5] F. Karsch, D. Kharzeev, H. Satz, Phys. Lett. B 637 (2006) 75.
- [6] G. Aad, et al., ATLAS Collaboration, Phys. Lett. B 697 (2011) 294.
- [7] S. Chatrchyan, et al., CMS Collaboration, J. High Energy Phys. 1205 (2012) 063.
- [8] B. Abelev, et al., ALICE Collaboration, Phys. Rev. Lett. 109 (2012) 072301.
- [9] C. Suiere, ALICE Collaboration, arXiv:1208.5601 [hep-ex]; A. Maire, ALICE Collaboration, arXiv:1301.4058 [hep-ex].

- [10] A. Adare, et al., PHENIX Collaboration, Phys. Rev. Lett. 98 (2007) 232301; A. Adare, et al., PHENIX Collaboration, Phys. Rev. C 84 (2011) 054912.
- [11] S. Chatrchyan, et al., CMS Collaboration, Phys. Rev. Lett. 109 (2012) 152303.
- [12] A. Andronic, P. Braun-Munzinger, K. Redlich, J. Stachel, Phys. Lett. B 652 (2007) 259.
- [13] X. Zhao, R. Rapp, Nucl. Phys. A 859 (2011) 114.
- [14] P. Bartalini, L. Fano, et al. (Eds.), Proceeds. MPI'08, arXiv:1003.4220 [hep-ex]; P. Bartalini, et al., Proceeds. MPI'11, arXiv:1111.0469 [hep-ph].
- [15] F. Abe, et al., CDF Collaboration, Phys. Rev. Lett. 79 (1997) 584.
- [16] V.M. Abazov, et al., DO Collaboration, Phys. Rev. D 81 (2010) 052012.
- [17] G. Aad, et al., ATLAS Collaboration, arXiv:1301.6872 [hep-ex]; CMS Collaboration, PAS-FSQ-12-028.
- [18] R. Aaij, et al., LHCb Collaboration, Phys. Lett. B 707 (2012) 52.
- [19] B. Abelev, et al., ALICE Collaboration, Phys. Lett. B 712 (2012) 165.
- [20] C.-H. Kom, A. Kulesza, W.J. Stirling, Phys. Rev. Lett. 107 (2011) 082002.
- [21] S.P. Baranov, A.M. Snigirev, N.P. Zotov, Phys. Lett. B 705 (2011) 116.
- [22] A.A. Novoselov, arXiv:1106.2184 [hep-ph].
- [23] S.P. Baranov, A.M. Snigirev, N.P. Zotov, A. Szczurek, W. Schafer, Phys. Rev. D 87 (2013) 034035.
- [24] D. d'Enterria, A.M. Snigirev, Phys. Lett. B 718 (2013) 1395.
- [25] M. Diehl, D. Ostermeier, A. Schafer, J. High Energy Phys. 1203 (2012) 089.
- [26] D. d'Enterria, arXiv:nucl-ex/0302016.
- [27] M. Strikman, D. Treleani, Phys. Rev. Lett. 88 (2002) 031801.
- [28] D. Treleani, G. Calucci, Phys. Rev. D 86 (2012) 036003.
- [29] C.W. deJager, H. deVries, C. deVries, At. Data Nucl. Data Tables 14 (1974) 485.
- [30] I.P. Lokhtin, A.M. Snigirev, Eur. Phys. J. C 16 (2000) 527.
- [31] R. Vogt, Phys. Rev. C 81 (2010) 044903.
- [32] K.J. Eskola, H. Paukkunen, C.A. Salgado, J. High Energy Phys. 0904 (2009) 065.
- [33] D. Acosta, et al., CDF Collaboration, Phys. Rev. D 71 (2005) 032001.
- [34] B. Abelev, et al., ALICE Collaboration, Phys. Lett. B 718 (2012) 295.
- [35] R. Aaij, et al., LHCb Collaboration, J. High Energy Phys. 1302 (2013) 041.
- [36] B. Abelev, et al., ALICE Collaboration, J. High Energy Phys. 1211 (2012) 065.
- [37] V. Khachatryan, et al., CMS Collaboration, Eur. Phys. J. C 71 (2011) 1575.
- [38] R. Aaij, et al., LHCb Collaboration, Eur. Phys. J. C 71 (2011) 1645.
- [39] F. Bossu, et al., arXiv:1103.2394 [nucl-ex].
- [40] R. Vogt, R.E. Nelson, A.D. Frawley, arXiv:1207.6812 [hep-ph].
- [41] E. Abbas, et al., ALICE Collaboration, arXiv:1305.1467 [nucl-ex].